

A Method for Reduction of Parallax Broadening in Gas-Based Position Sensitive Detectors

P. Rehak, *Member, IEEE*, G.C. Smith, *Member, IEEE* and B. Yu
Brookhaven National Laboratory, Upton, NY 11973-5000

Abstract

A description is given of the principle and experimental verification of a new method which significantly reduces broadening of the position response, due to parallax, for radiation incident on a detector at finite angles of incidence. The technique, which can be implemented in gas-based position-sensitive detectors with planar geometry, substantially improves position resolution for scattering experiments using X-rays and neutrons, and will permit larger angular coverage than has previously been possible. An improvement of nearly a factor four in rms position resolution is predicted, which is confirmed by measurements using a gas proportional X-ray detector with delay-line position encoding.

I. INTRODUCTION

Structural studies of samples in a number of disciplines, such as molecular biology, solid state physics and material science, are frequently made by using X-ray and neutron scattering, especially with the monochromatic, high fluxes available at synchrotron sources (X-rays) and reactors/spallation sources (neutrons). Typically, these studies involve the measurement of diffraction patterns with position sensitive detectors. In specific biological studies, polymer research and, particularly, sub-second time resolved studies, gas-based proportional detectors play a vital role [1,2]. While these devices can be fabricated in a wide range of collecting areas, they can only be conveniently made in planar geometry. Since they require an absorbing region of typically a centimeter of gas in order to achieve good detection efficiency, the position response can

be significantly broadened when radiation enters at finite angles of incidence. This phenomenon has, to some extent, limited the application of gas-based detectors.

Only a small number of previous studies have been made by other groups to alleviate the effects of parallax. At CERN, a cone-shaped drift region was installed above a conventional two-dimensional chamber to create the spherical drift chamber [3]. A version of this detector has been used for protein crystallography at LURE [4]; this is the only one known to the authors that has been so applied. A method developed by Breskin et al. [5] involved weighting the position of a recorded event according to its pulse height from a parallel plate avalanche detector, but we are unaware of applications of this method. A detector marketed by Siemens [6] has a drift region which is bounded on the entrance side with a spherical window, and by a planar cathode at the rear. In short, there are few examples of gas-based detectors with any parallax reduction because of the significant fabrication difficulties entailed. We describe here a new method that greatly reduces the effects of parallax broadening, and which is specifically designed for existing planar two-dimensional chambers.

II. OUTLINE OF PRINCIPLE

Usually, an imaging gas detector has two regions where the conversion of X-rays occurs. The major one is the absorption and drift region, depth t , between the window and cathode wire plane (figure 1); the second region is that between the two cathodes (depth $2d$), where d is the anode-

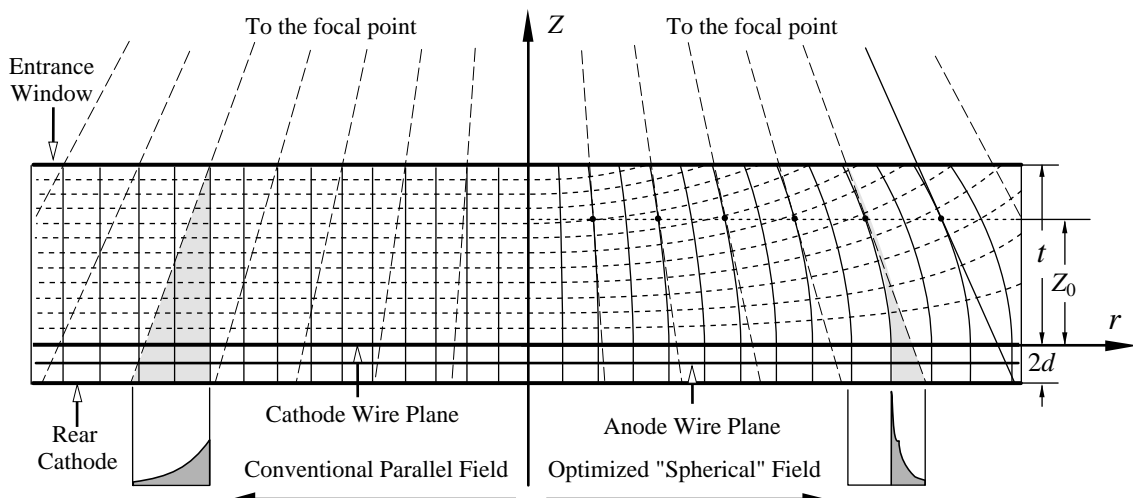


Figure 1. Plan view which illustrates X-ray (or neutron) radiation, scattered from a sample at the focal point, incident on a gas proportional chamber. The left hand side represents the parallel field produced by a conventional, uniform potential window, yielding significant parallax error, while the right hand side shows the 'spherical' field produced by a new window design, with which parallax error is significantly reduced.

cathode spacing. In practice, the detector is designed such that the majority of photons are absorbed in the drift region.

Parallax broadening in a conventional gas detector occurs in the parallel field of the complete depth of the detector, where signal electrons always drift perpendicularly to the electrodes; this is shown in the left hand side of figure 1. To eliminate parallax, signal electrons should move along radial lines which intercept at a point coinciding with the position of the sample under study. This focal point is a distance f from the cathode wire plane. Such an ideal, parallax free, field is spherical and is that which would be produced by a point charge located at the sample position. If the entrance window and the cathode wire plane were held at the potential of the spherical field at their respective locations, the electric field in the drift region would be spherical and electrons would move along the parallax-free lines. In practice, it is very hard to apply a variable potential to the cathode wire plane, but the potential of the entrance window can be changed in a radially symmetric way to minimize the effect of parallax. The resulting field is shown in the right hand side of the detector in figure 1.

The cathode wire plane, at $Z = 0$, is an equipotential surface, and therefore field lines must intercept it at right angles, corresponding to a focal point at infinity. With increasing Z , the field lines start to bend toward the center line of the detector; at a distance Z_0 , the tangents to the field lines intersect exactly the focal point, or sample position. Due to the nature of the electrostatics, the field lines continue to curve and the tangents to the lines for $Z > Z_0$ intersect closer than the focal point. It can be shown that each field line is closely approximated by a parabola, completely defined by its point of origin at the plane $Z = 0$, (where its derivative is zero), and the location of the tangent that intersects the focal point. Assuming that signal electrons drift along these lines of force, it is possible to calculate their spread in arrival position at the anode plane by appropriately weighting the X-ray conversion point with λ , the X-ray absorption length in the gas. Figure 2 shows this spread as a function of Z_0 for three different incident angles. We see that there is a value of Z_0 for which the spread is a

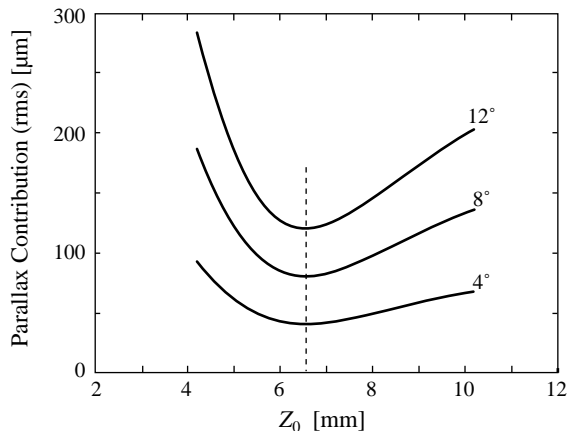


Figure 2. Parallax contribution vs. Z_0 , where Z_0 is the azimuthal position in the detector at which the tangent to the drift field line intersects the sample position, or focal point.

minimum; furthermore this value is practically independent of the incident angle of the radiation. The value of Z_0 , which depends upon λ , f , t and d , defines the geometry of the electric field lines in the volume between the entrance window and the cathode wire plane. A family of curves, perpendicular everywhere to the field lines, defines lines of equipotential (shown in the right hand side of the detector in figure 1), and is similar to a family of concentric circles which would correspond to an ideal spherical field.

The value of the electric potential at the central line of the detector ($r = 0$) was taken as the potential of an imaginary dipole field which produces the required focusing effect in a region close to this central line. The values of the potential from this line were carried to the entrance window by the family of equipotential lines, thus defining the required potential on the entrance window. The resulting potential has a profile which is approximately Gaussian with

$$\sigma = \sqrt{f \cdot Z_0} \quad (1).$$

III. EXPERIMENTAL SETUP

An initial set of measurements has been performed using a two-dimensional multi-wire chamber that our group has already built for X-ray diffraction experiments using synchrotron radiation. This detector has the following characteristics: a beryllium entrance window with an area of $10\text{cm} \times 10\text{cm}$, a drift depth, $t = 10.2\text{mm}$, and a multi-wire structure with half gap $d = 1.25\text{mm}$, resulting in a total gas depth of 12.7mm . Position readout is accomplished by an optimized delay line on each of the cathodes. (An earlier version of this detector has been described in reference [1].)

The beryllium window has been replaced by one which creates the 'spherical' field. It has been fabricated using standard photolithography and evaporated aluminum to form concentric, conducting annuli on a $50\mu\text{m}$ mylar sheet. A thin layer of chromium is deposited on the clear mylar before the aluminum to prevent charging up of the exposed areas. The voltage profile on the annuli has been optimized according to eq.(1) for these initial tests for $f = 18\text{cm}$ and $\lambda = 2.5\text{mm}$, which corresponds to the absorption depth of 5.4keV radiation and a mixture of $\text{Xe}/10\%\text{CO}_2$ at atmospheric pressure. This gas mixture is one which is used routinely in scattering experiments, and the radiation is conveniently generated from a sealed tube with a chromium anode.

The window pattern produced for this work is shown in figure 3. There are sixty annuli, about the maximum that can be created across the 10cm diameter while maintaining good edge definition of each annulus. The pitch of the annuli is tailored such that a voltage divider comprising equal value resistors generates the correct Gaussian potential profile on the window; the resistor network was constructed on an adjoining printed circuit board, figure 3. Clearly this particular window design means at least one quarter of the detector area is unusable, and that part used for our tests is highlighted; our

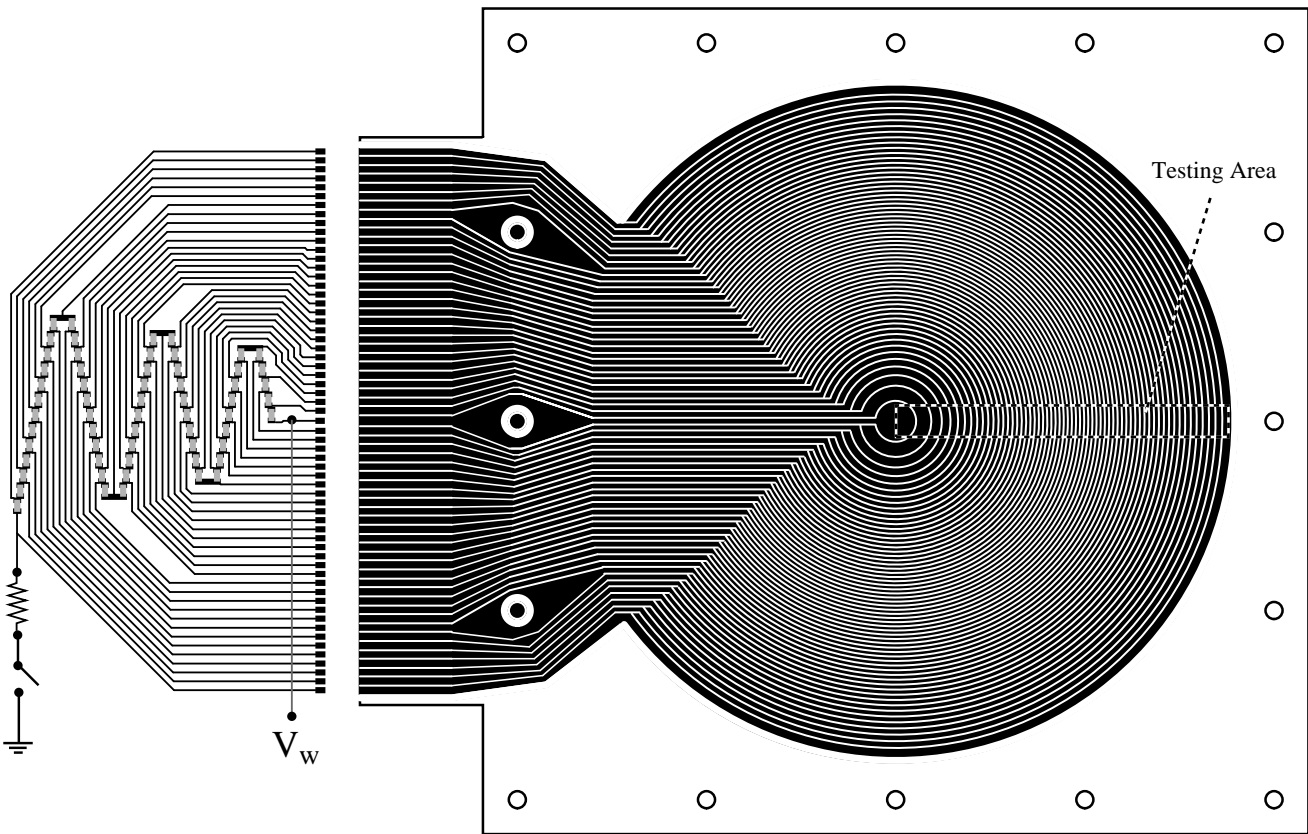


Figure 3. Conducting pattern on detector entrance window used in present measurements. Window material is mylar sheet, with conducting annuli (black) from evaporated aluminum. The resistive divider at left applies potential which varies from 2.5kV on the central disc to 500V on the outer annulus.

aim was to ensure correct application of voltage to each annulus and this method proved very effective.

A particularly important feature of the test window design is that a parallel field can be created in the drift region by just removing the low voltage end of the resistive divider, figure 3, from ground. This allows comparison of the detector response with parallel field, and a 'spherical' field, with no physical change or movement in the experimental setup.

An X-ray beam collimated to $25\mu\text{m}$ was incident on the detector, which was placed 18cm from the X-ray source, or focal point. The detector could be rotated accurately about the focal point, an angular range of zero to 12° being achievable with this arrangement.

IV. RESULTS

The spectra with thick lines in figure 4 show the detector position response to collimated X-rays as a function of X-ray incident angle, for a parallel field in the drift region; each position peak has been normalized to the same number of counts. At zero degrees, the FWHM resolution is $120\mu\text{m}$, consistent with previous measurements using this detector system [1]; this value is due to the combined contributions of photoelectron range [7], electron diffusion and electronic noise. As the incident angle increases, the FWHM becomes progressively larger because of parallax, and at 12° has in-

creased to $600\mu\text{m}$; this latter value is wholly dominated by parallax. In many X-ray scattering experiments, diffraction peaks are accompanied by a uniform background of diffusely scattered radiation, and this figure illustrates how a diffraction peak would eventually merge with the background at larger angles of incidence.

The spectra with thin lines in figure 4 show the seven corresponding position profiles (again, normalized to the same number of counts) for a 'spherical' field in the drift region; the improvement is very marked. At an angle as large as 12° , the FWHM is now only $180\mu\text{m}$, and as a consequence the peak intensity is a factor four greater than for the parallel field. Clearly, if this were a diffraction peak it would now be much more easily discernible from any diffuse background.

An important feature of the optimization described in section 2 is the fact that the shape and value of the 'spherical' field is accurately known. It is therefore possible to calculate the expected point response of the detector at any incident angle. It is straightforward also to calculate the point response for the normal parallel field condition. Figure 5(a) shows the calculated point response for the present experimental conditions for an incident angle of 12° ; note the logarithmic scale on the ordinate. Exponential absorption for the parallel field case yields the widest of the two curves. The curve for the 'spherical field' is clearly much narrower; the direct overlap

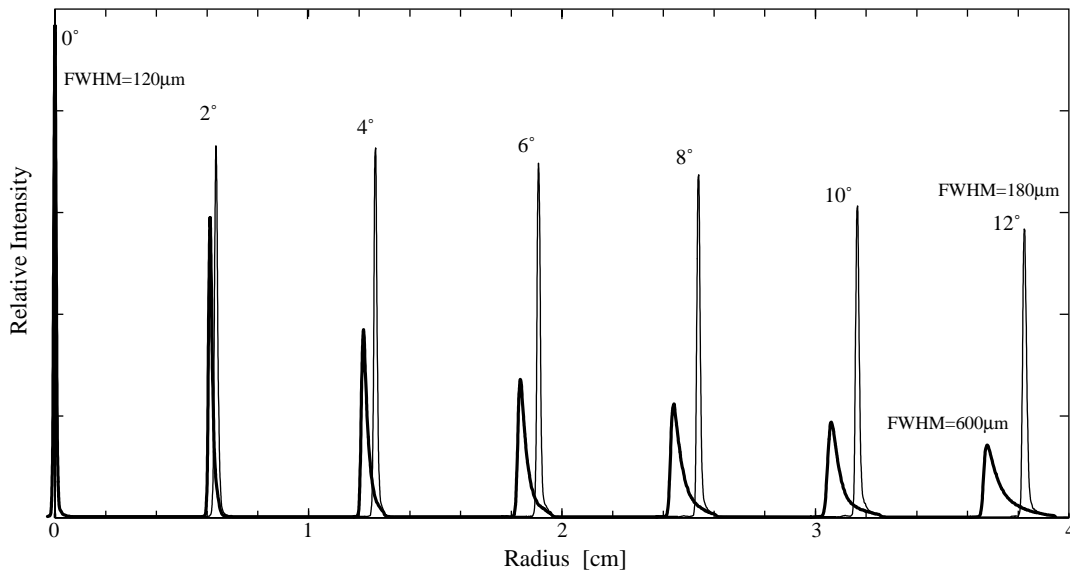


Figure 4. Position response of detector to $25\mu\text{m}$ wide X-ray beams, incident on the entrance window over the range of 0° (normal incidence at center) to 12° (near edge of detector). Thick lines represent parallel field in the drift region, and thin lines represent the new 'spherical' field. All peaks are normalized to the same number of counts.

of the two curves at the right hand side of the figure corresponds to X-rays absorbed between the two cathodes. Figure 5(b) shows the corresponding experimental distributions, which are just expansions of the two 12° curves in figure 4. The agreement between experiment and simulation is excellent.

From the simulation, it is possible to calculate an improvement factor of the 'spherical' field performance compared to the parallel field. However, the simulation only takes account of parallax, and, experimentally, the improvement factor is influenced by other phenomena, especially at angles of incidence very close to normal. The predicted resolution due to parallax alone has therefore been added quadratically to a detector response of $50\mu\text{m}$ rms. The curve in figure 6 shows the improvement factor for angles up to 12° , together with corresponding experimental values. Again the agreement is excellent.

An unwanted side-effect resulting from the 'spherical' field in the drift region is an anode gain dependence on position in the detector. There is a small degree of 'field leakage' from the multiplication region between the two cathodes, into the drift region, because of the transparency of the cathode wire plane. Thus the field at the surface of a specific anode wire is influenced to a minor extent by the field directly above it in the drift region. Figure 7 shows the measured anode gain dependence as a function of drift field; the field change in the test detector is represented by the continuous curve; for completeness, the dashed curve continues to higher and lower fields. The gain change over the face of the detector is therefore a little under 20%, which contributes to a slight broadening of the anode pulse height spectrum. This, in turn, is reflected in the cathode signal amplitudes, but for most position encoding systems, including the delay-line readout used here, the absolute position scale is not sensitive to such changes in gas gain.

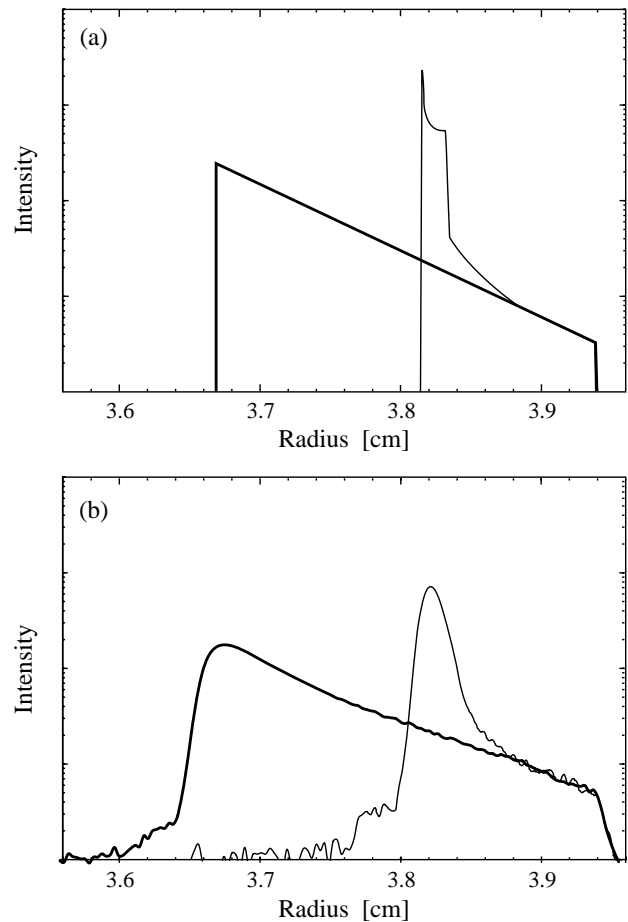


Figure 5. Position response of detector to X-ray beams incident at 12° , near edge of detector. Thick lines represent 'parallel' field in the drift region, and thin lines represent the new 'spherical' field. (a) represents simulation of infinitely narrow beam, (b) shows measurements with a $25\mu\text{m}$ wide X-ray beam.

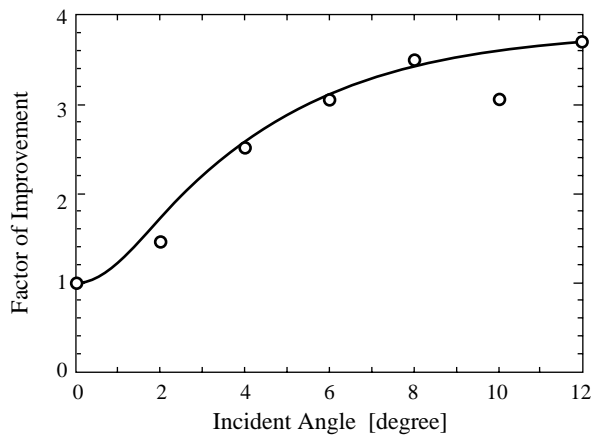


Figure 6. Diagram to show the factor of improvement of a detector with a 'spherical' drift field over that with a parallel drift field. Continuous curve is simulation, circles are measurements.

V. DISCUSSION

Improvements in position resolution of up to nearly a factor four have been demonstrated by this new parallax reducing technique. In principle, it is easier to implement than previous methods that have been used to combat parallax, and it can be adapted to existing planar detectors. It is equally applicable to one-dimensional detectors (with suitably biased parallel, conducting strips on the window). It may be feasible with this technique to accommodate more than one focal length with a single window by adjustment of potentials on the window annuli, offering the possibility of software controllable focal length.

Obviously, the present window design would not be used in a practical detector because it does not provide the correct 'spherical' field over the entire area. We are currently investigating techniques to provide the desired voltage profile on a mylar window with full annuli.

This technique is suitable for both neutron and X-ray instrumentation. For neutron detectors a window may be easily fabricated from printed circuit board with virtually no influence on neutron transmission; thus, by using multi-layer circuit board technology, it will be simple to apply voltage to the central electrode. High precision thermal neutron detectors have been made for some years by our group [2], and we are preparing to apply this technique to neutron instrumentation.

The field leakage from drift region to multiplication region results in a minor degradation to the energy resolution because of gas gain variation.

This new technique offers the prospect of improving the position resolution of all gas-filled imaging devices, with little change to the physical structure of the detector, permitting the recording of accurate diffraction data over significantly larger angles than has previously been possible.

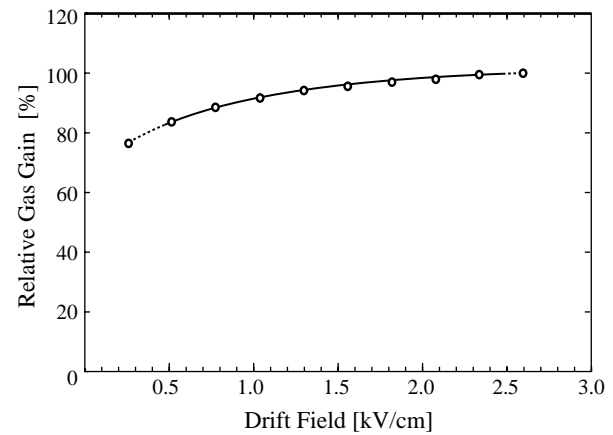


Figure 7. Variation of gas gain with value of drift field. The drift field in the test detector varies from approximately 2.5 kV/cm in the center to 500V/cm at the edge.

VI. ACKNOWLEDGMENTS

We would like to acknowledge discussions with Prof. Emilio Gatti (Polytechnic Institute of Milan) concerning the electrostatics of the detector drift field. We would like to thank Gene Von Achen for his skill in assembling the detector and Bob Di Nardo for the window vacuum evaporation. This work was supported by the U. S. Department of Energy under Contract No. DE-AC02-76CH00016.

VII. REFERENCES

- [1] M.S. Capel, G.C. Smith and B. Yu, "One- and two-dimensional x-ray detector systems at NSLS beam line X12B, for time-resolved and static x-ray-diffraction studies," *Rev. Sci. Instr.* **66** (1995) 2330-2332.
- [2] V. Radeka, N. Schaknowski, G.C. Smith and B. Yu, "High precision thermal neutron detectors," in *Neutrons in Biology*, ed. B. Schoenborn & R.B. Knott, Plenum Press (in press).
- [3] G. Charpak, Z. Hajduk, A. Jeavons, R. Stubbs and R. Khan, "The spherical drift chamber for X-ray imaging applications," *Nucl. Instr. & Meth.* **122** (1974) 307-312.
- [4] R. Kahn, R. Fourme, R. Bosshard and V. Saintagne, "An area-detector diffractometer for the collection of high resolution and multiwavelength anomalous diffraction data in macromolecular crystallography," *Nucl. Instr. & Meth.* **A246** (1986) 596-603.
- [5] A. Breskin, G. Charpak and J.C. Santiard, "A multistep parallax-free X-ray imaging counter," *Nucl. Instr. & Meth.* **195** (1982) 469-473.
- [6] HI-STAR Area Detector, Siemens Analytical X-ray Systems, Inc.
- [7] J. Fischer, V. Radeka and G.C. Smith, "X-ray position detection in the region of 6 μ m rms with wire proportional chambers," *Nucl. Instr. & Meth.* **A252** (1986) 239-245.